

Multi-objective Model-Predictive Control for Dielectric Elastomer Wave Harvesters.

Matthias K. Hoffmann* Lennart Heib* Gianluca Rizzello**
Giacomo Moretti*** Kathrin Flaßkamp*

* *Systems Modeling and Simulation,*
(e-mail: {matthias.hoffmann, kathrin.flaskkamp}@uni-saarland.de,
lennartheib@gmail.com)

** *Intelligent Material Systems Lab,*
(e-mail: gianluca.rizzello@imsl.uni-saarland.de)

*** *Università degli Studi di Trento, (e-mail: giacomo.moretti@unitn.it)*
* and ** from Saarland University, Saarbrücken, Germany.

Abstract:

Keywords: Multi-objective Optimal Control, Model-predictive Control, Energy Harvesting, Non-Linear Optimization, Dielectric Elastomer Generators

1. INTRODUCTION

2. MODEL AND PROBLEM STATEMENT

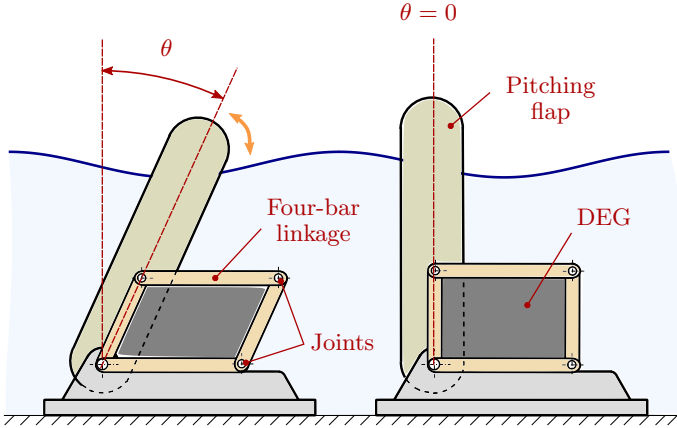


Fig. 1. Wave surge converter: A flap mounted to the sea floor is tilted by the wave motion. It is displayed in a generic (left) and the vertical equilibrium position (right).

2.1 Background

Model-predictive Control (MPC) arose from optimal control as one answer on how to “close the loop” (Rawlings et al. (2017)). In optimal control, a system’s behaviour is predicted for a time called the prediction horizon t_f into the future, while optimising the inputs to the system, such that a cost function is minimised. The working principle of MPC is repeatedly measuring the system’s state, solving an Optimal Control Problem (OCP), and applying the first few of the calculated inputs.

2.2 System

In this work, we investigate the MPC of the wave surge converter (see, e.g. Whittaker and Folley (2012)), dis-

played in Fig. 1. The device is pivoted to the sea, such that incoming waves excite an oscillatory motion. This distorts a dielectric elastomer generator (DEG) mounted to a deformable parallelogram, Moretti et al. (2014). Through this parallelogram, the DEG applies a torque to the flap towards the equilibrium position $\theta = 0$. Applying a voltage to the DEG adds an electrostatically-induced torque in the same angular direction, making the system stiffer.

When a voltage is applied to the DEG, charge carriers accumulate in the DEG. By deforming the parallelogram to a smaller area (increased θ), the charge density increases, such that energy can be extracted. As we showed in our previous work Hoffmann et al. (2022), controlling the input to maximise the energy extracted from the system requires application of large voltages, damaging the DEG-material over time, and resulting in system failure after too much damage accumulated Chen et al. (2019). For that reason, we also took the damage into consideration as a second control goal, resulting in lower electric fields in the DEG.

2.3 Model

The dynamics of the wave surge

$$\begin{aligned} \begin{bmatrix} \dot{\theta} \\ \dot{\delta} \\ \dot{z} \end{bmatrix} &= \begin{bmatrix} 0 & 1 & 0^{1 \times n} \\ -I_h^{-1}K_h & -I_h^{-1}B_h & -I_h^{-1}C_r \\ 0^{n \times 1} & B_r & A_r \end{bmatrix} \begin{bmatrix} \theta \\ \delta \\ z \end{bmatrix} + \\ &+ \begin{bmatrix} 0 \\ I_h^{-1} \\ 0^{n \times 1} \end{bmatrix} (d - C_0\theta u) \end{aligned} \quad (1)$$

$$\theta(0) = \theta_0, \delta(0) = \delta_0, z(0) = z_0,$$

contain the equation of angular motion and the wave loads generated by the interaction of the waves with the flap. Here, $\delta = \dot{\theta}$ describes the flap’s angular velocity, $z \in \mathbb{R}^n$ the n -dimensional state vector for wave radiation (Yu and Falnes (1995)) and d the force the waves exert on the flap. The input u is the electrostatic force generated by the DEG when a voltage v is applied. Since the DEG’s

electrostatic force is proportional to the v^2 , u is restricted to be positive. [add u constraint explanation?](#)

$$u \leq (E_{bd}h_l)^2 / \cos^2(\theta), \quad (2)$$

2.4 Cost functions

Our aim is the simultaneous minimisation of damage and maximisation of extracted energy, which we will employ in a multi-objective Optimal Control (MOOCP) setting. The extracted energy cost function is modelled as the negative generated energy

$$J_1 = \Psi(t_f) - \Psi(0) + \int_0^{t_f} \left(B_h \delta^2 + z^\top S_r z + \frac{u}{R_0} - d\delta \right) dt$$

with $\Psi = \frac{1}{2}I_h \delta^2 + \frac{1}{2}K_h \theta^2 + \frac{1}{2}z^\top Q_r z + \frac{1}{2}C_0(1 - \theta^2)u$, (3)

with the storage function Ψ including kinematic, potential, electrostatic, and hydrodynamic energy contributions. Dissipations due to viscous, hydrodynamic, and electrical losses, and the power input by the incident wave are considered via the integral terms.

Under the assumption, that damage only starts accumulating after the applied electric field exceeds a threshold E_{th} , the cost function can be formulated as

$$J_2 = \alpha \int_0^{t_f} \left(\max\{\cos^2(\theta)u - E_{th}^2 h_l^2, 0\} \right)^{n_d} dt, \quad (4)$$

with a normalisation factor α rendering J_2 dimensionless, and an experimental parameter n_d . [too close to Mathmod paper?](#)

Equations (1), (2), (3), and (4) formulate the MOOCP

Problem 1.

$$\begin{aligned} & \underset{u(t)}{\text{minimize}} && (J_1, J_2) \\ & \text{subject to dynamics (1)} \\ & && 0 \leq \cos^2(\theta)u \leq (E_{bd}h_l)^2. \end{aligned} \quad (5)$$

that is solved inside the MPC.

3. METHODS

3.1 Discretisation and simplification of the OCP

In order to solve the Problem 1, we employ direct methods for optimal control to first formulate the OCP as a non-linear program (NLP) (see Gerdt (2011)). Using gradient-based methods, the discretised optimal control sequence is calculated. The integral terms inside the cost functions have to be approximated. We do so by adding the integrand to the dynamics

$$\begin{aligned} \dot{\Upsilon}_1 &= B_h \delta^2 + z^\top S_r z + \frac{u}{R_0} - d\delta \\ \dot{\Upsilon}_2 &= (\max\{u - E_{th}^2 h_l^2, 0\})^{n_d}, \end{aligned}$$

with

$$\Upsilon_1(0) = \Upsilon_2(0) = 0.$$

Remark, that the term $\cos^2(\theta)$ is simplified to 1, the same is done in the constraint on u . The extended state

reads $\xi = [\theta \ \vartheta \ z^\top \ \Upsilon_1 \ \Upsilon_2]^\top$, with the initial value $\xi_0 = [\theta_0 \ \vartheta_0 \ z_0^\top \ 0 \ 0]^\top$

In the following, the discretised values corresponding to their continuous counterparts are marked by square brackets, e.g. the state vector $\xi[k]$, the extended state k time steps into the future. The current state of the system is advanced by one step into the future using the classical Runge-Kutta-Method of 4-th order (RK4), denoted by $F_{RK4}(\xi[k], u[k], u[k+1], d[k], d[k+1])$. Consecutive values for the input and wave excitation are used to model first-order hold behaviour. The dynamics can then be expressed with the equality constraints

$$\begin{aligned} \xi[k+1] &= F_{RK4}(\xi[k], u[k], u[k+1], d[k], d[k+1]) \\ &\quad \forall k \in [0, N-2] \\ \xi[0] &= \xi_0, \end{aligned}$$

where N is the number of time steps t_f is separated into. The cost functions are then $J_1 \approx \Upsilon_1[N-1]$ and $J_2 \approx \Psi[N-1] - \Psi[0] + \Upsilon_2[N-1]$, so that the MOOCP is

Problem 2.

$$\begin{aligned} & \underset{u[1], \dots, u[N]}{\text{minimize}} && w_1 J_1 + w_2 J_2 \\ & \text{subject to} && \xi[k+1] = F_{RK4}(\xi[k], u[k], u[k+1], \dots \\ & && d[k]), d[k+1]) \forall k \in [0, N-2], \\ & && 0 \leq u[k] \leq (E_{bd}h_l)^2, \forall k \in [0, N-1] \quad (6) \\ & && \xi[0] = \xi_0 \quad (7) \\ & && u[0] = u_0, \quad (8) \end{aligned}$$

where u_0 is a fixed initial value of 0 and especially for $k > 0$ u_0 is the previous step's $u[1]$ [hier mpc notation sinnvoll...](#)

3.2 Wave generation

3.3 Adaptive weight selection

When applying MPC, we do not know exactly how the system will perform over the deployment of the control. In the case of the WEC-DEG when driving the system with a set weighting, different sea states will result in a different damage accumulation over time. Since the DEG has to be replaced once it breaks down, an operator of multiple DEGs might be interested replacing all of the devices at the same time to save monetary costs. This means, that the breakdown of all the devices has to be synced, e.g. by changing the weighting of the damage cost function in a way, such that the accumulated damage cost at the designated break-down time t_{bd} does not exceed a fixed value J^d .

Assume a fixed set w of n_w weight combinations sorted from low to high priority for the handled cost function (in our case J_2) and an initial weight index $i_w \in [1, n_w]$. One easy way of deciding, if the damage goal is achievable with the current weighting is by evaluating the MPC performance over N_p time steps into the past. The average rate of damage accumulation J_{ps} is estimated and the damage at the break-down time is predicted as an average trend. This is done every N_p steps. Algorithm 1 shows the selection, where k is the current time step.

[is probably not necessary with the repo](#)

For an exemplary implementation in MATLAB using our system, refer to [link](#).

Algorithm 1: Weight selection for i -th cost function

Input: $J^d, t_{bd}, i_w, n_w, J_i^r, \mu_d, N_p, \Delta t, k$ **Output:** i_w

```
if  $k + 1 \bmod N_p = 0$  then
     $J_{ps} \leftarrow \frac{1}{N_p \Delta t} \sum_{l=0}^{N_p-1} J_i^r[k-l]$ ;
    if  $\sum_{l=0}^j + J_{ps}(t_{bd} - k\Delta t) > J^d$  and  $i_w < n_w$  then
        |  $i_w = i_w + 1$ 
    else if  $\sum_{l=0}^j + J_{ps}(t_{bd} - k\Delta t) > J^d$  and  $i_w > 1$ 
        then
            |  $i_w = i_w - 1$ 
    end
end
```

4. NUMERICAL RESULTS

The following simulations were done using MATLAB. The optimisation problems were formulated and solved using the CasADi package by Andersson et al. (2019) and the Ipopt solver by Wächter and Biegler (2006).

4.1 Multi-objective Optimal Control

Methods from Hoffmann et al. (2022).

4.2 Model-predictive Control

5. CONCLUSION

REFERENCES

- Andersson, J.A., Gillis, J., Horn, G., Rawlings, J.B., and Diehl, M. (2019). Casadi: a software framework for nonlinear optimization and optimal control. *Mathematical Programming Computation*, 11(1), 1–36. doi: 10.1007/s12532-018-0139-4.
- Chen, Y., Agostini, L., Moretti, G., Berselli, G., Fontana, M., and Vertechy, R. (2019). Fatigue life performances of silicone elastomer membranes for dielectric elastomer transducers: preliminary results. In *Electroactive Polymer Actuators and Devices (EAPAD) XXI*, volume 10966, 1096616. International Society for Optics and Photonics.
- Gerdts, M. (2011). *Optimal Control of ODEs and DAEs*. Walter de Gruyter.
- Hoffmann, M.K., Moretti, G., Rizzello, G., and Flaßkamp, K. (2022). Multi-objective optimal control for energy extraction and lifetime maximisation in dielectric elastomer wave energy converters. *IFAC-PapersOnLine*, 55(20), 546–551.
- Moretti, G., Forehand, D., Vertechy, R., Fontana, M., and Ingram, D. (2014). Modeling of an oscillating wave surge converter with dielectric elastomer power take-off. In *International Conference on Offshore Mechanics and Arctic Engineering*, volume 45530, V09AT09A034. American Society of Mechanical Engineers.
- Rawlings, J.B., Mayne, D.Q., and Diehl, M. (2017). *Model predictive control: theory, computation, and design*, volume 2. Nob Hill Publishing Madison, WI.
- Wächter, A. and Biegler, L.T. (2006). On the implementation of an interior-point filter line-search algorithm for large-scale nonlinear programming. *Mathematical programming*, 106(1), 25–57.
- Whittaker, T. and Folley, M. (2012). Nearshore oscillating wave surge converters and the development of oyster. *Philosophical Transactions of the Royal Society A: Mathematical, Physical and Engineering Sciences*, 370(1959), 345–364.
- Yu, Z. and Falnes, J. (1995). State-space modelling of a vertical cylinder in heave. *Applied Ocean Research*, 17(5), 265–275.